Chapter 2
Bifurcations and Chaos in Dynamical Systems

Complex systems theory deals with dynamical systems containing often large numbers of variables. It extends dynamical systems theory, which treats dynamical systems containing a few variables. A good understanding of dynamical systems theory is therefore a prerequisite when studying complex systems.

In this chapter we introduce core concepts, like attractors and Lyapunov exponents, bifurcations, and deterministic chaos from the realm of dynamical systems theory. An introduction to catastrophe theory will be provided together with the notion of rate-induced tipping and colliding attractors.

Most of the chapter will be devoted to ordinary differential equations and maps, the traditional focus of dynamical systems theory, venturing however towards the end into the intricacies of time delay dynamical systems.

2.1 Basic Concepts of Dynamical Systems Theory

Dynamical systems theory deals with the properties of coupled differential equations, determining the time evolution of a few, typically a handful of variables. We present a concise overview covering the most important concepts and phenomena.

Fixpoints and Limit Cycles In order to illustrate methodologies typical for dynamical systems theory, we start with an elementary non-linear rotator. For a two-dimensional systems $\mathbf{x} = (x, y)$, or

$$x(t) = r(t)\cos(\varphi(t)), \qquad y(t) = r(t)\sin(\varphi(t)) \tag{2.1}$$

in polar coordinates, we postulate the non-linear differential equations

$$\dot{r} = (\Gamma - r^2)\, r, \qquad \dot{\varphi} = \omega \tag{2.2}$$

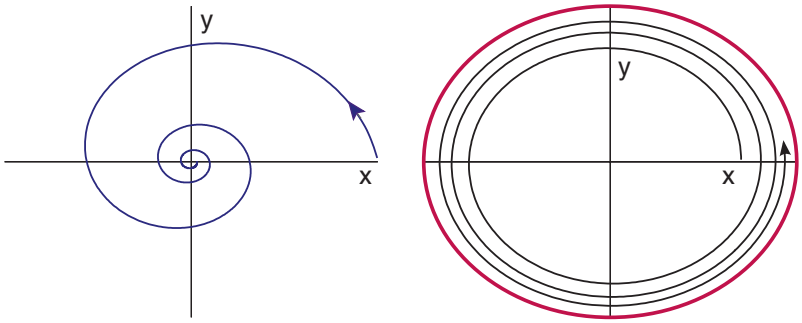

Fig. 2.1 The solution of the non-linear rotator, compare (2.1) and (2.2). For $\Gamma < 0$ the orbit is attracted by a stable fixpoint (left), for $\Gamma > 0$ by a stable limit cycle (right).

govern the dynamical behavior. The typical orbits $(x(t), y(t))$ are illustrated in Fig. 2.1. The limiting behavior of (2.2) is

$$\lim_{t\to\infty} \begin{bmatrix} x(t) \\ y(t) \end{bmatrix} = \begin{cases} \begin{bmatrix} 0 \\ 0 \end{bmatrix} & \Gamma < 0 \\ \begin{bmatrix} r_c \cos(\omega t) \\ r_c \sin(\omega t) \end{bmatrix} & r_c^2 = \Gamma > 0 \end{cases} \tag{2.3}$$

In the first case, $\Gamma < 0$, trajectories are attracted by the stable fixpoint $\mathbf{x}_0^* = (0, 0)$. In the second case, $\Gamma > 0$, the dynamics approaches stable periodic orbit.

LIMIT CYCLE Trajectories retrace themselves with a period T for limit cycles, viz one has $\mathbf{x}(t + T) = \mathbf{x}(t)$.

Limit cycles can be attracting or repelling. In (2.3) one has an attracting limit cycle for $\Gamma > 0$.

Bifurcation Of particular interest are situations where the behavior of a dynamical system changes qualitatively.

BIFURCATION The long-term limiting behavior of a dynamical system described by a set of parameterized differential equations may change qualitatively as a function of an external parameter. The resulting change in terms of fixpoints, limit cycles and/or chaotic attractors constitutes a bifurcation.

The dynamical system (2.1) and (2.2) shows a bifurcation at $\Gamma = 0$, at which a fixpoint turns into a limit cycle. One denotes this specific type of bifurcation a "Hopf bifurcation", as discussed lateron in detail

Stability of Fixpoints The dynamics of orbits close to fixpoints or limiting orbits is determined by its stability.

STABILITY CONDITION A fixpoint is stable (unstable) if nearby orbits are attracted (repelled) by the fixpoint, and metastable if the distance does not change.

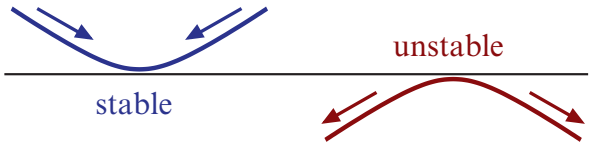

Fig. 2.2 A fixpoint is stable (unstable) when orbits are attracted (repelled).

An illustration is given in Fig. 2.2. The stability of fixpoints is closely related to their Lyapunov exponents, as discussed in Sect. 2.4.

One can examine the stability of a fixpoint $\mathbf{x}^*$ by linearizing the equation of motions for $\mathbf{x} \approx \mathbf{x}^*$. For the fixpoint $r^* = 0$ of (2.2) we find

$$\dot{r} = \left(\Gamma - r^2\right) r \approx \Gamma r, \qquad r \ll 1\,,$$

and $r(t)$ decreases (increases) for $\Gamma < 0$ ($\Gamma > 0$). For a d-dimensional system $\mathbf{x} = (x_1, \ldots, x_d)$ the stability of a fixpoint $\mathbf{x}^*$ is determined by calculating the d eigenvalues of the linearized equations of motion. The system is stable if all eigenvalues are negative and unstable if at least one eigenvalue is positive.

Phase Space A given dynamical systems lives in its phase space.

> Phase Space The phase space is the space spanned by all allowed values of the variables entering a set of first-order differential equations defining the dynamical system.

For a two-dimensional system (x, y) the phase space is $\mathbb{R}^2$, but in the polar coordinates one has

$$\left\{ (r, \varphi) \,\middle|\, r \in [0, \infty],\ \varphi \in [0, 2\pi[\right\}.$$

The representation of a phase space changes upon coordinate transformations.

Attracting States and Manifolds Attracting states play a center role in dynamical systems theory.

> Attractor A bounded region in phase space to which orbits with certain initial conditions come arbitrarily close is called an attractor.

Attractors can be isolated points, fixpoints, limit cycles or more complex objects like attracting manifolds, viz subsets of phase space, or chaotic attractors.

> Basin of Attraction The set of initial conditions in phase space leading to orbits approaching a certain attractor arbitrarily closely is the basin of attraction.

Most of the times the extend of a basin of attraction can be evaluated only numerically.

First-Order Differential Equations Let us consider the third-order differential equation

$$\frac{d^3}{\mathrm{d}t^3}x(t) = f(x, \dot{x}, \ddot{x})\,. \tag{2.4}$$

Using

$$x_1(t) = x(t), \qquad x_2(t) = \dot{x}(t), \qquad x_3(t) = \ddot{x}(t)\,, \tag{2.5}$$

we can rewrite (2.4) as a first-order differential equation,

$$\frac{\mathrm{d}}{\mathrm{d}t}\begin{bmatrix} x_1 \\ x_2 \\ x_3 \end{bmatrix} = \begin{bmatrix} x_2 \\ x_3 \\ f(x_1, x_2, x_3) \end{bmatrix}\,.$$

One can reduce any set of coupled differential equations to a set of first-order differential equations by introducing an appropriate number of additional variables. We therefore consider in the following only first-order, ordinary differential equations.

Autonomous Systems The generic form for a dynamical system is

$$\frac{\mathrm{d}\mathbf{x}(t)}{\mathrm{d}t} = \mathbf{f}(\mathbf{x}(t)), \qquad \mathbf{x}, \mathbf{f} \in \mathbb{R}^d, \qquad t \in [-\infty, +\infty]\,, \tag{2.6}$$

when time is continuous, or, equivalently, maps such as

$$\mathbf{x}(t+1) = \mathbf{g}(\mathbf{x}(t)), \qquad \mathbf{x}, \mathbf{g} \in \mathbb{R}^d, \qquad t = 0, 1, 2, \ldots\,, \tag{2.7}$$

when time is discrete. Together with the time evolution equation one has to set the initial condition $\mathbf{x}_0 = \mathbf{x}(t_0)$. An evolution equation of type (2.15) is denoted "autonomous", since it does not contain an explicit time dependence. A system of type $\dot{\mathbf{x}} = \mathbf{f}(t, \mathbf{x})$ is dubbed "non-autonomous".

A particular solution $\mathbf{x}(t)$ of a dynamical system in phase space is denoted "trajectory", or "orbit". Orbits are uniquely determined by the set of initial conditions, $\mathbf{x}(0) \equiv \mathbf{x}_0$, a consequence of dealing with first-order differential equations.

Poincaré Map It is in general difficult to illustrate graphically the motion of $\mathbf{x}(t)$ in d dimensions. Our retina, as well as our print media, are two-dimensional and it is therefore convenient at times to consider a plane Σ in $\mathbb{R}^d$ together with the points $\mathbf{x}^{(i)}$ marking the consecutive intersections of an orbit with Σ, as illustrated in Fig. 2.3. As an example consider the plane

$$\Sigma = \{\, (x_1, x_2, 0, \ldots, 0) \,|\, x_1, x_2 \in \mathbb{R} \,\}$$

and the sequence of intersections (see Fig. 2.3)

$$\mathbf{x}^{(i)} = (x_1^{(i)}, x_2^{(i)}, 0, \ldots, 0), \qquad (i = 1, 2, \ldots)$$

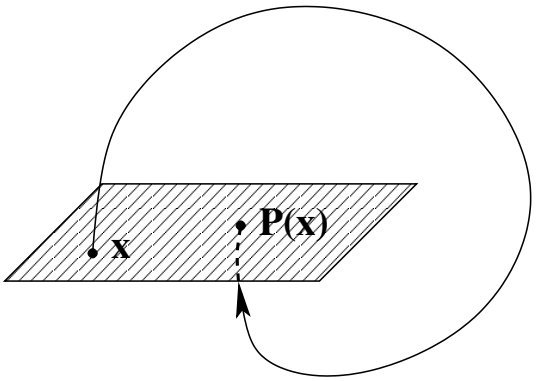

Fig. 2.3 The Poincaré map, $\mathbf{x} \to \mathbf{P}(\mathbf{x})$, which maps an intersection $\mathbf{x}$ of the trajectory with a hyperplane (shaded) to the consecutive intersection $\mathbf{P}(\mathbf{x})$.

which define the "Poincaré map"

$$\mathbf{P}: \ \mathbf{x}^{(i)} \ \mapsto \ \mathbf{x}^{(i+1)} \,. \tag{2.8}$$

The Poincaré map is a discrete map, compare (2.7), which can be constructed for continuous-time dynamical systems like (2.15). The Poincaré map is very useful, since we can print and analyze it directly. In the simplest case, a periodic orbit would show up in the Poincaré map as the identity mapping.

Constants of Motion and Ergodicity Dynamical systems derived in physics from Hamilton- or Lagrange formalism are "mechanical systems". The vast majority of dynamical systems we will examine are non-mechanical. There are however several foundational concepts from the realm of mechanical systems that are generically relevant.

– Constant of Motion
  A function $F(\mathbf{x})$ on phase space $\mathbf{x} = (x_1, \ldots, x_d)$ is a "constant of motion" if it is conserved under the time evolution of the dynamical system, i.e. when
  $$\frac{\mathrm{d}}{\mathrm{d}t} F(\mathbf{x}(t)) = \sum_{i=1}^{d} \left(\frac{\partial}{\partial x_i} F(\mathbf{x}) \right) \dot{x}_i(t) \equiv 0$$
  holds for all times t. In many mechanical systems the energy is a conserved quantity.
– Ergodicity
  A dynamical system in which orbits come arbitrarily close to any allowed point in the phase space, irrespective of the initial condition, is called ergodic.

All conserving systems of classical mechanics are ergodic. The ergodicity of a mechanical system is closely related to "Liouville's theorem".[1]

[1] Liouville's theorem will be discussed in Sect. **??** of Chap. **??**, "**??**".

Ergodicity holds only modulo conserved quantities, which is the case for the energy in many mechanical systems. Then, only points in the phase space having the same energy as the trajectory considered are approached arbitrarily close. It is clear that ergodicity and attractors are mutually exclusive: An ergodic system cannot have attractors and a dynamical system with one or more attractors cannot be ergodic.

Mechanical Systems and Integrability A dynamical system of type

$$\ddot{x}_i = f_i(\boldsymbol{x}, \dot{\boldsymbol{x}}), \qquad i = 1, \ldots, f$$

is a mechanical system, since equations of motion in classical mechanics are of this form, e.g. Newton's law. f is called the degree of freedom, which implies that mechanical systems can be written as a set of coupled first-order differential equations with $2f$ variables constituting the phase space,

$$(x_1 \ldots x_f, v_1 \ldots v_f), \qquad v_i = \dot{x}_i, \qquad i = 1, \ldots, f\,,$$

with $\mathbf{v} = (v_1, \ldots, v_f)$ being the generalized velocity. A mechanical system is "integrable" if there are $\alpha = 1, \ldots, f$ independent constants of motion $F_\alpha(\boldsymbol{x}, \dot{\boldsymbol{x}})$, such that

$$\frac{d}{\mathrm{d}t} F_\alpha(\boldsymbol{x}, \dot{\boldsymbol{x}}) = 0, \qquad \alpha = 1, \ldots, f\,.$$

The motion in the $2f$-dimensional phase space $(x_1 \ldots x_f, v_1 \ldots v_f)$ is then restricted to an f-dimensional subspace, which is an f-dimensional torus, see Fig. 2.4.

An example of an integrable mechanical system is the Kepler problem, viz the motion of earth around the sun. Integrable systems are very rare, they constitute however important reference points for the understanding of more complex dynamical systems. A classical example of a non-integrable mechanical system is the three-body problem, viz the combined motion of earth, moon and sun around each other.

KAM Theorem Kolmogorov, Arnold and Moser (KAM) examined the question of what happens to an integrable system when it is perturbed. Let us consider a two-dimensional torus, as illustrated in Fig. 2.4. Orbit wraps around the torus respectively with frequencies ω_1 and ω_2. A key quantity is the ratio of revolution frequencies ω_1/ω_2, which can be rational or irrational.

We recalr that irrational numbers r may be approximated with arbitrary accuracy by a sequence of quotients

$$\frac{m_1}{s_1}, \ \frac{m_2}{s_2}, \ \frac{m_3}{s_3}, \ \ldots \qquad\qquad s_1 < s_2 < s_3 < \ldots$$

with ever larger denominators s_i. A number r is "very irrational" when it is difficult to approximate r by such a series of rational numbers, viz when

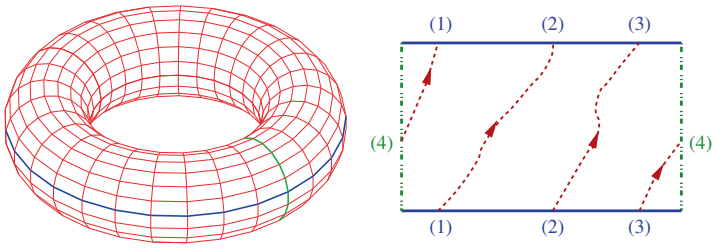

Fig. 2.4 Left: A KAM-torus can be cut along two lines (vertical/horizontal) and unfolded. **Right:** A closed orbit on the unfolded torus with $\omega_1/\omega_2 = 3/1$. The numbers indicate points that coincide after refolding (periodic boundary conditions).

very large denominators s_i are required to achieve a certain given accuracy for $|r - m/s|$.

The KAM theorem states that orbits with rational ratios of revolution frequencies ω_1/ω_2 are the most unstable under a perturbation of an integrable system and that tori are most stable when this ratio is very irrational.

Gaps in the Saturn Rings A spectacular example for the instability of rational KAM-tori are the gaps in the rings of the planet Saturn.

The time a hypothetical particle in Cassini's gap (between the A- and the B-ring, $r = 118,000\,\mathrm{km}$) would need to orbit Saturn is half the orbiting period of the 'shepherd-moon' Mimas. The quotient of these two revolving frequencies is 2:1. Particle orbiting in Cassini's gap are therefore unstable against perturbation caused by Mimas and thrown out of their orbit.

2.2 Fixpoints, Bifurcations and Stability

We start our systematic discussions by considering the stability of fixpoint x^* of a one-dimensional dynamical system

$$\dot{x} = f(x), \qquad f(x^*) = 0\,. \tag{2.9}$$

A fixpoint is the most simplest invariant manifold.[2] Generically, invariant manifolds are sets of phase space that that are invariant under the dynamical flow.

Fixpoints are the only possible invariant manifolds for $d = 1$ dimension, in two dimensions fixpoints and limiting cycles are possible, with more complicated objects, such as strange attractors, becoming accessible in three and higher dimensions.

[2] Invariant manifolds are touched upon further in in Sect. **??** of Chap. **??**, "**??**".

Lyapunov Exponents The stability of a fixpoint is determined by the direction of the flow close to it, which can be determined by linearizing the time evolution equation $\dot{x} = f(x)$ around the fixpoint x^*,

$$\frac{d}{dt}\big(x - x^*\big) = \dot{x} \approx f(x^*) \,+\, f'(x^*)(x - x^*) \,+\, \dots\,, \tag{2.10}$$

where $f'()$ denotes the first derivative. We rewrite (2.10) as

$$\frac{d}{dt}\Delta x = f'(x^*)\,\Delta x, \qquad\qquad \Delta x = x - x^*\,,$$

where we neglected terms of order $(x - x^*)^2$ and higher and where we made use of the fixpoint condition $f(x^*) = 0$. This equation has the solution

$$\Delta x(t) = \Delta x(0)\,\mathrm{e}^{t f'(x^*)} \quad\to\quad \begin{cases} \infty & f'(x^*) > 0 \\ 0 & f'(x^*) < 0 \end{cases}\,. \tag{2.11}$$

The perturbation Δx decreases/increases with time and the fixpoint x^* is hence stable/unstable for $f'(x^*) < 0$ and $f'(x^*) > 0$ respectively.

LYAPUNOV EXPONENT The time evolution close to a fixpoint x^* is generically exponential, $\sim \exp(\lambda t)$, and one denotes by $\lambda = f'(x^*)$ the Lyapunov exponent.

The Lyapunov exponent controls the direction of the flow close to a fixpoint. Orbits are exponentially repelled/attracted for $\lambda > 0$ and for $\lambda < 0$ respectively. For more than a single variable one has to find all eigenvalues of the linearized problem, as discussed further below, with the fixpoint being stable only when all eigenvalues are negative.

Fixpoints of Discrete Maps For a discrete map of type

$$x(t+1) = g(x(t)), \qquad\qquad x^* = g(x^*) \tag{2.12}$$

the stability of a fixpoint x^* can be determined by an equivalent linear analysis,

$$x(t+1) = g(x(t)) \approx g(x^*) \,+\, g'(x^*)(x(t) - x^*)\,.$$

Using the fixpoint condition $g(x^*) = x^*$ we write above expression as

$$\Delta x(t+1) = x(t+1) - x^* = g'(x^*)\,\Delta x(t)\,,$$

which has the solution

$$\Delta x(t) = \Delta x(0)\,\big[g'(x^*)\big]^t, \qquad\qquad |\Delta x(t)| = |\Delta x(0)|\,\mathrm{e}^{\lambda t}\,. \tag{2.13}$$

The Lyapunov exponent,

$$\lambda = \log|g'(x^*)| = \begin{cases} < 0 & \text{for} \quad |g'(x^*)| < 1 \\ > 0 & \text{for} \quad |g'(x^*)| > 1 \end{cases}\,, \tag{2.14}$$

controls the stability of the fixpoint. Note the differences in the relation of the Lyapunov exponent λ to the derivatives $f'(x^*)$ and $g'(x^*)$ for differential equations and maps respectively, as given by (2.11) and (2.14).

2.2.1 Fixpoints Classification and Jacobian

We assume that the general d-dimensional dynamical system

$$\frac{\mathrm{d}\mathbf{x}(t)}{\mathrm{d}t} = \mathbf{f}(\mathbf{x}(t)), \qquad \mathbf{x}, \mathbf{f} \in \mathbb{R}^d, \qquad \mathbf{f}(\mathbf{x}^*) = 0 \tag{2.15}$$

has a fixpoint $\mathbf{x}^*$.

Jacobian and Lyapunov Exponents For a stability analysis of the fixpoint $\mathbf{x}^*$ one linearizes (2.15) around the fixpoint, using $x_i(t) \approx x_i^* + \delta x_i(t)$, with small $\delta x_i(t)$. One obtains

$$\frac{d\delta x_i}{dt} = \sum_j J_{ij}\, \delta x_j, \qquad J_{ij} = \left.\frac{\partial f_i(x)}{\partial x_j}\right|_{\mathbf{x}=\mathbf{x}^*}. \tag{2.16}$$

The matrix J_{ij} of all possible partial derivatives is the "Jacobian" of the dynamical system (2.15). The Jacobian allows to generalizes the definition of the Lyapunov exponent for one-dimensional systems, as given previously.

LYAPUNOV SPECTRUM The set of eigenvalues $\{\lambda_i\}$ of the Jacobian $i = 1, .., d$ is the spectrum characterizing the fixpoint $\mathbf{x}^*$.

Lyapunov exponents $\lambda_n = \lambda'_n + i\lambda''_n$ may have real λ'_n and imaginary λ''_n components, which leads to the time evolution

$$\mathrm{e}^{\lambda_n t} = \mathrm{e}^{\lambda'_n t}\, \mathrm{e}^{i\lambda''_n t}$$

of infinitesimal perturbations around the fixpoint. A Lyapunov exponent λ_n is attracting/neutral/repelling when λ'_n is negative/zero/positive respectively.

HYPERBOLIC FIXPOINT The flow is well defined in linear order when all $\lambda'_i \neq 0$. In this case the fixpoint is hyperbolic.

For a non-hyperbolic fixpoint at least one of the Lyapunov exponents is neutral. All Lyapunov exponents are neutral for a vanishing Jacobian.

Pairwise Conjugate Exponents With $\lambda = \lambda' + i\lambda''$ also its conjugate $\lambda^* = \lambda' - i\lambda''$ in an eigenvalue of the Jacobian, which is a real matrix. It follows that λ and λ^* differ when $\lambda'' \neq 0$. In this caser there are (at least) two eigenvalues having the same real part λ'.

Fixpoint Classification for $d = 2$ In Fig. 2.5 some example trajectories are shown for several fixpoints in $d = 2$ dimensions.

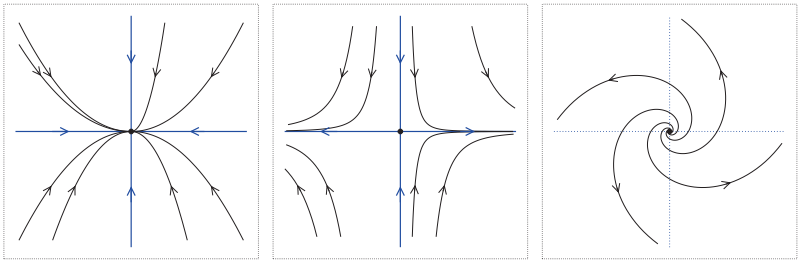

Fig. 2.5 Example trajectories for a stable node (left), with a ratio $\lambda_2/\lambda_1 = 2$, for a saddle (middle) with $\lambda_2/\lambda_1 = -3$, and for a unstable focus (right).

- Node
  Both eigenvalues are real and have the same sign, which is negative/positive for a stable/unstable node.
- Saddle
  Both eigenvalues are real and have opposite signs.
- Focus
  The eigenvalues are complex conjugate to each other. The trajectories spiral in/out for negative/positive real parts.

Fixpoints in higher dimensions are characterized by the number of respective attracting/neutral/repelling eigenvalues of the Jacobian, which may be in turn either real or complex.

Stable and Unstable Manifolds For real eigenvalues $\lambda_n \neq 0$ of the Jacobian J, with eigenvectors $\mathbf{e}_n$ and a sign $s_n = \lambda_n/|\lambda_n|$, we define via

$$\lim_{t \to -s_n \infty} \mathbf{x}_n(t) = \mathbf{x}^* + \mathrm{e}^{t\lambda_n}\mathbf{e}_n, \qquad J\mathbf{e}_n = \lambda_n \mathbf{e}_n\,, \tag{2.17}$$

trajectories $\mathbf{x}_n(t)$ that leave/approach the fixpoint parallel to an eigendirection. These are stable manifolds (for $\lambda_n < 0$) and unstable manifolds (for $\lambda_n > 0$).

For a neutral Lyapunov exponent with $\lambda_n = 0$ one define a "center manifold" which we will discuss in the context of catastrophe theory in Sect. 2.3.2. The term manifold denotes in mathematics, loosely speaking, a smooth topological object.

Stable and unstable manifolds control the flow infinitesimal close to the fixpoint along the eigendirections of the Jacobian and may be continued to all positive and negative times t. Typical examples are illustrated in Figs. 2.5 and 2.6.

Heteroclinic orbits One speaks of a "heteroclinc orbit" when the unstable manifold of one fixpoint connects to the stable manifold of another fixpoint, and viceversa. As an example, we consider a two dimensional dynamical system defined by

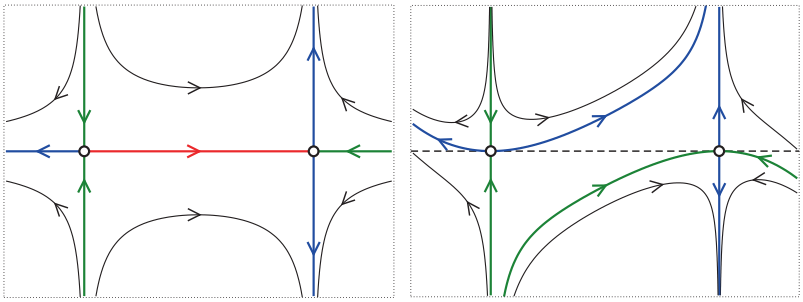

Fig. 2.6 Sample trajectories of the system (2.18), for $\epsilon = 0$ (left) and $\epsilon = 0.2$ (right). Shown are the stable manifolds (thick green lines), the unstable manifolds (thick blue lines) and the heteroclinic orbit (thick red line).

$$\begin{aligned} \dot{x} &= 1 - x^2 \\ \dot{y} &= yx + \epsilon\big(1 - x^2\big)^2 \end{aligned} \qquad J(x^*) = \begin{pmatrix} -2x^* & 0 \\ 0 & x^* \end{pmatrix}, \tag{2.18}$$

which has two saddles $\mathbf{x}^*_\pm = (x^*, 0)$, where $x^* = \pm 1$. The eigenvectors of the Jacobian $J(x^*)$ are aligned with the x and the y axis respectively, for all values of the control parameter ϵ.

The flow diagram, as illustrated in Fig. 2.6, is invariant when inverting both $x \leftrightarrow (-x)$ and $y \leftrightarrow (-y)$. The system contains additionally the $y = 0$ axis as a mirror line for a vanishing $\epsilon = 0$ and there is a heteroclinic orbit connecting an unstable manifold of $\mathbf{x}^*_-$ to one of the stable manifolds of $\mathbf{x}^*_+$. A finite ϵ removes the mirror line $y = 0$, present at $\epsilon = 0$, destroying the heteroclinic orbit. Real world systems are often devoid of symmetries and heteroclinic orbits hence rare.

2.2.2 Bifurcations and Normal Forms

The nature of the solution to a dynamical system, as defined by a suitable first order differential equation (2.15), may change qualitatively as a function of a given control parameter. When this happens, a bifurcation occurs. Here we list the most important classes of what is called a "local bifurcation". The distinction to their counterpart, "global bifurcations", will be elucidated in Sect. 2.3.

A local bifurcations can be characterized by a simple archetypical equation, the "normal form", to which a more complex dynamical systems will generically reduce close to the transition point.

Saddle-node Bifurcation We consider the dynamical system defined by

$$\frac{dx}{dt} = a - x^2\,, \tag{2.19}$$

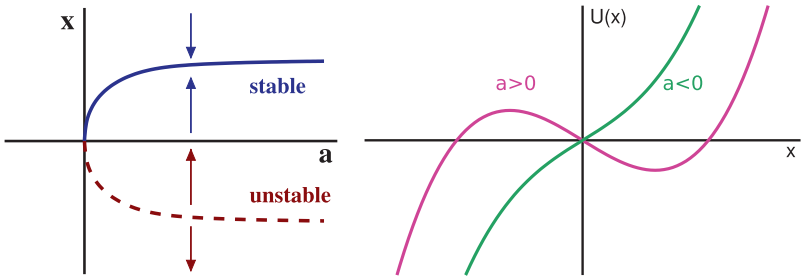

Fig. 2.7 The saddle-node bifurcation, as described by (2.19). There are two fixpoints for $a > 0$, an unstable branch $x^*_- = -\sqrt{a}$ and a stable branch $x^*_+ = +\sqrt{a}$. **Left:** The phase diagram together with the flow (arrows). **Right:** The bifurcation potential $U(x) = -ax + x^3/3$, compare (2.26).

for a real variable x and a real control parameter a. The fixpoints $\dot{x} = 0$

$$x^*_+ = +\sqrt{a}, \qquad x^*_- = -\sqrt{a}, \qquad a > 0 \tag{2.20}$$

exist only for positive control parameters, $a > 0$; there are no fixpoints for negative $a < 0$. For the flow we find

$$\frac{dx}{dt} = \begin{cases} < 0 & \text{for} \quad x > \sqrt{a} \\ > 0 & \text{for} \quad x \in [-\sqrt{a}, \sqrt{a}] \\ < 0 & \text{for} \quad x < -\sqrt{a} \end{cases} \tag{2.21}$$

when $a > 0$. The upper branch x^*_+ is hence stable and the lower branch x^*_- unstable, as illustrated in Fig. 2.7.

For a saddle-node bifurcation a stable and an unstable fixpoint collide and annihilate each other, one speaks also of a fold, tangential or blue sky bifurcation.

Transcritical Bifurcation We now consider the dynamical system

$$\frac{dx}{dt} = x(a - x)\,, \tag{2.22}$$

again for a real variable x and a real control parameter a. The two fixpoint solutions $\dot{x} = 0$,

$$x^*_0 = 0, \qquad x^*_a = a, \qquad \forall a \tag{2.23}$$

exist for all values of the control parameter. The direction of the flow $\dot{x}$ is positive for x in between the two solutions and negative otherwise, see Fig. 2.8. The respective stabilities of the two fixpoint solutions exchange consequently at $a = 0$.

Pitchfork Bifurcation The "supercritical" pitchfork bifurcation is described by

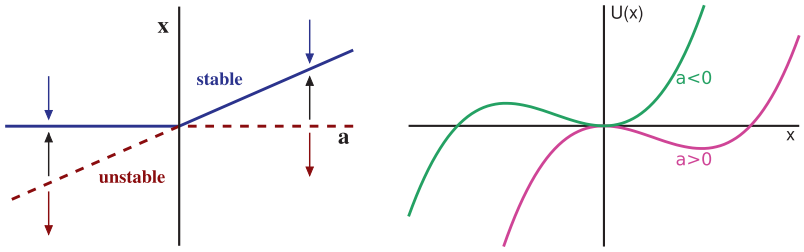

Fig. 2.8 The transcritical bifurcation, see (2.22). The two fixpoints $x_0^* = 0$ and $x_a^* = a$ exchange stability at $a = 0$. **Left:** Phase diagram and flow (arrows). **Right:** The bifurcation potential $U(x) = -ax^2/2 + x^3/3$, compare (2.26).

$$\frac{dx}{dt} = ax - x^3, \qquad x_0^* = 0, \qquad x_+^* = +\sqrt{a}, \qquad x_-^* = -\sqrt{a}\,. \tag{2.24}$$

The trivial fixpoint $x_0^* = 0$ becomes unstable at criticality, $a = 0$, and two symmetric stable fixpoints appear, see Fig. 2.9.

Bifurcation Potentials In many cases one can write the dynamical system under consideration as

$$\frac{dx}{dt} = -\frac{d}{dx}\,U(x)\,, \tag{2.25}$$

where $U(x)$ is a potential in analogy to Newton's equation of motion in classical mechanics. Local minima of the potential correspond to stable fixpoints, compare Fig. 2.2. The potentials for the saddle-node and the transcritical bifurcation are

$$U_{\rm saddle}(x) = -ax + \frac{1}{3}x^3, \qquad U_{\rm trans}(x) = -\frac{a}{2}x^2 + \frac{1}{3}x^3\,, \tag{2.26}$$

respectively, see the definitions (2.19) and (2.22). The bifurcation potentials, as shown in Figs. 2.7 and 2.8, bring immediately to evidence the stability of the respective fixpoints. The bifurcation potential of the pitchfork bifuration,

$$U_{\rm pitch}(x) = -\frac{a}{2}x^2 + \frac{1}{4}x^4\,, \tag{2.27}$$

is identical to the Landau-Ginzburg potential describing second-order phase transitions in statistical physics.[3] Of relevance is also the subcritical pitchfork transition, defined by $\dot{x} = ax + x^3$.

Bifurcation Symmetries The three bifurcation scenarios discussed above, saddle-node, transcritical and pitchfork, are characterized by their symmetries close to the critical point, which has been set to $x = 0$ and $a = 0$ in all three cases. The normal forms and their respective bifurcation potentials

[3] The Landau-Ginzburg theory of phase transitions will be treated at length in the context of self-organized criticality, in Sect. **??**. of Chap. **??**, "**??**".

constitute the simplest formulations consistent with the defining symmetry properties.

The bifurcation potentials of the saddle-node and the pitchfork transitions are respectively antisymmetric and symmetric under a sign change $x \leftrightarrow -x$ of the dynamical variable, compare (2.26) and (2.27).

$(+) \leftrightarrow (-)$	saddle-node	transcritical	pitchfork
x	anti	–	symm
a, x	–	anti	–

The bifurcation potential of the transcritical bifurcation is, on the other hand, antisymmetric under the combined symmetry operation $x \leftrightarrow -x$ and $a \leftrightarrow -a$, compare (2.26).

2.2.3 Hopf Bifurcations and Limit Cycles

Hopf Bifurcation A Hopf bifurcation occurs when a fixpoint changes its stability together with the appearance of an either stable or unstable limiting cycle, e.g. as for non-linear rotator illustrated in Fig. 2.1. The canonical equations of motion are[4]

$$\begin{aligned} \dot{x} &= -y + d(\Gamma - x^2 - y^2)\, x \\ \dot{y} &= x + d(\Gamma - x^2 - y^2)\, y \end{aligned} \tag{2.28}$$

in Euclidean phase space $(x, y) = (r\cos\varphi, r\sin\varphi)$. The standard non-linear rotator (2.2) is recovered when setting $d = 1$. There are two steady-state solutions for $\Gamma > 0$,

$$(x_0^*, y_0^*) = (0, 0), \qquad (x_\Gamma^*, y_\Gamma^*) = \sqrt{\Gamma}\,(\cos(t), \sin(t))\,, \tag{2.29}$$

a fixpoint and a limit cycle. The limit cycle disappears for $\Gamma < 0$.

Super- vs. Sub-critical Hopf Bifurcation For $d > 0$ the bifurcation is "supercritical". The fixpoint $\mathbf{x}_0^* = (x_0^*, y_0^*)$ is stable/unstable for $\Gamma < 0$ and $\Gamma > 0$ and the limit cycle $\mathbf{x}_\Gamma^* = (x_\Gamma^*, y_\Gamma^*)$ is stable, as illustrated in Fig. 2.1.

The direction of flow is reversed for $d < 0$, with the limit cycle $\mathbf{x}_\Gamma^*$ becoming repelling. The fixpoint $\mathbf{x}_0^*$ is then unstable/stable for $\Gamma < 0$ and $\Gamma > 0$ and one speaks of a "subcritical" Hopf bifurcation.

Hopf Bifurcation Theorem One may be interested to find out whether a generic two dimensional system,

$$\dot{x} = f_\mu(x, y), \qquad \dot{y} = g_\mu(x, y)\,, \tag{2.30}$$

[4] In complex plane, with $z = x + iy$, Eq. (2.28) takes the form of a Stuart–Landau oscillator, $\dot{z} = i\omega z + d(\Gamma - |z|^2)z$, with $\omega = 1$.

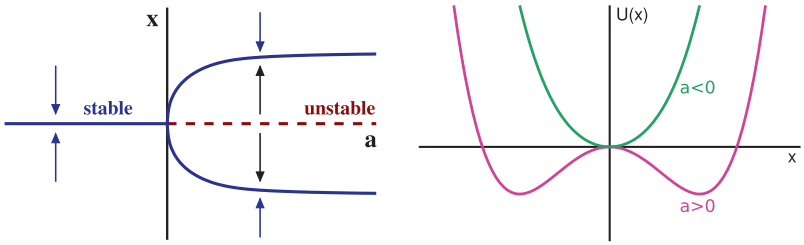

Fig. 2.9 The supercritical pitchfork bifurcation, as defined by (2.24). The t$x_0^* = 0$ becomes unstable for $a > 0$ and two new stable fixpoints, $x_+^* = +\sqrt{a}$ and $x_-^* = -\sqrt{a}$ appear. **Left:** Phase diagram and flow (arrows). **Right:** The bifurcation potential $U(x) = -ax^2/2 + x^4/4$, compare (2.26).

can be reduced to the normal form (2.28) for a Hopf bifurcation, where μ is the bifurcation parameter. Without loss of generality one can assume that the fixpoint $\mathbf{x}_0^*$ stays at the origin for all values of μ and that the transition takes place for $\mu = 0$.

To linear order the normal form (2.28) and (2.30) are equivalent if the Jacobian of (2.30) has a pair of complex conjugate eigenvalues, with the real value crossing $\mu = 0$ with a finite slope, which corresponds to a transition from a stable to an unstable focus.

Comparing (2.28) and (2.30) to quadratic order one notices that quadratic terms are absent in the normal form (2.28) but not in (2.30). One can however show, with the help of a suitable non-linear transformation, that it is possible to eliminate all quadratic terms from (2.30). One finds that the nature of the bifurcation is determined by a combination of partial derivatives up to cubic order,

$$\begin{aligned} a = &\big[f_{xxx} + f_{xyy} + g_{xxy} + g_{yyy}\big]/16 \\ &+ \big[f_{xy}(f_{xx} + f_{yy}) - g_{xy}(g_{xx} + g_{yy}) - f_{xx}g_{xx} - f_{yy}g_{yy}\big]/(16\omega) \end{aligned}$$

where $\omega > 0$ is the imaginary part of the Lyapunov exponent at the critical point $\mu = 0$ and where the partial derivatives as f_{xy} are to be evaluated at $\mu = 0$ and $\mathbf{x} \to \mathbf{x}_0^*$. The Hopf bifurcations is supercritical and subcritical respectively for $a < 0$ and $a > 0$.

Interplay Between Multiple Limit Cycles A dynamical system may dispose of a number of distinct limit cycles, which can merge or disappear as a function of a given parameter. We consider the simplest case, generalizing the non-linear rotator (2.2) to the next order in r^2,

$$\dot{r} = -(r^2 - \gamma_-)(r^2 - \gamma_+)\, r, \qquad \dot{\varphi} = \omega, \qquad \gamma_- \le \gamma_+ \,. \tag{2.31}$$

Real-world physical or biological systems have bounded trajectories, which implies that $\dot{r}$ must be negative for large radii $r \to \infty$. This requirement has been taken into account in (2.31), the "Bautin normal form".

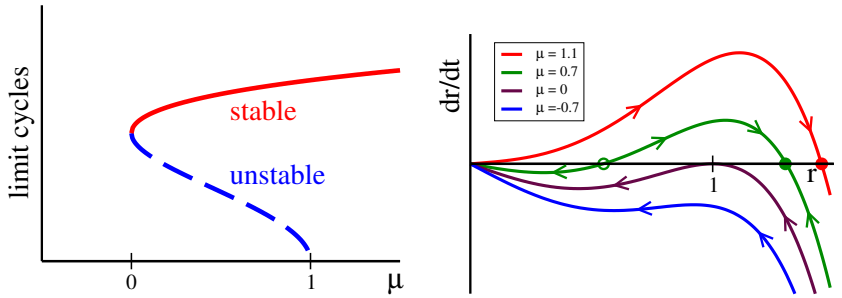

Fig. 2.10 Left: For a fold bifurcation of limit cycles, the locations $R_\pm = \sqrt{1 \pm \sqrt{\mu}}$ of the stable and unstable limit cycles, R_- and R_+, as defined by (2.31) and (2.32). At $\mu = 0$ a fold bifurcation of limit cycles occurs and a subcritical Hopf bifurcation at $\mu = 1$. **Right:** The respective flow diagram. The filled/open circles denote stable/unstable limit cycles. For $\mu \to 1$ the unstable limit cycle vanishes, a subcritical Hopf bifurcation. The stable and the unstable limit cycle collided for positive $\mu \to 0$ and annihilate each other, a fold bifurcation of limit cycles.

For $\gamma_- < 0$ the first factor $(r^2 - \gamma_-)$ is smooth for $r^2 \geq 0$ and does not influence the dynamics qualitatively. In this case (2.31) reduces to a standard supercritical Hopf bifurcation, as a function of the bifurcation parameter γ_+.

Phenomenological Parametrization The roots $\gamma_\pm$ of r^2 in (2.31) typically result from some determining relation. As a possible simple assumption we consider the form

$$\gamma_\pm = 1 \pm \sqrt{\mu}\,, \tag{2.32}$$

where μ will be our bifurcation parameter. For $\mu \in [0, 1]$ we have two positive roots and consequently also two limit cycles, a stable and an unstable one. For $\mu \to 1$ the unstable limit cycle vanishes in a subcritical Hopf bifurcation, compare Fig. 2.10.

Fold Bifurcation of Limit Cycles For a saddle-node bifurcation of fixpoints, aka fold bifurcation, a stable and an unstable fixpoint merge and annihilate each other, as illustrated in Fig. 2.7. The equivalent phenomenon occurs for limit cycles, as shown in Fig. 2.10, happening in our model when μ becomes negative,

$$\gamma_\pm = 1 \pm i\sqrt{|\mu|}, \qquad \dot{r} = -\big[(r^2 - 1)^2 + |\mu|\big] r\,.$$

No limit cycle exists for $\mu \leq 0$, only a stable fixpoint at $r_0^* = 0$ remains.

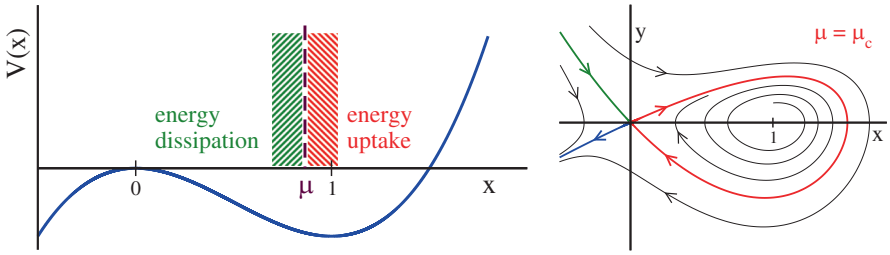

Fig. 2.11 Left: The potential $V(x)$ of the Taken–Bogdanov system (2.33). Energy is dissipated to the environment for $x < \mu$ and taken up for $x > \mu$. For $\mu < 1$ the local minimum $x = 1$ of the potential becomes an unstable focus. **Right:** The flow for the critical $\mu = \mu_c \approx 0.8645$. The stable and unstable manifolds form an homoclinic loop (red line).

2.3 Global Bifurcations

The bifurcations discussed in Sect. 2.2 are termed "local" as they are based on Taylor expansions around a local fixpoint, which implies that the dynamical state changes smoothly at the bifurcation point. There are, on the other hand, bifurcations characterized by the properties of extended orbits. These kinds of bifurcations are hence of "global" character.

Taken–Bogdanov System We consider a mechanical system with a cubic potential $V(x)$ and velocity-dependent forces,

$$\begin{array}{ll} \ddot{x} = (x-\mu)\dot{x} - V'(x) & \dot{x} = y \\ V(x) = x^3/3 - x^2/2 & \dot{y} = (x-\mu)y + x(1-x) \end{array} . \tag{2.33}$$

The conservative contribution to the force is $-V'(x) = x(1-x)$, as illustrated in Fig. 2.11. The energy, defined by

$$E = \frac{\dot{x}^2}{2} + V(x), \qquad \frac{dE}{dt} = \left[\ddot{x} + V'(x)\right]\dot{x} = (x-\mu)\dot{x}^2 , \tag{2.34}$$

is dissipated when $x < \mu$, viz when the term $(x-\mu)\dot{x}$ in (2.33) reduces the velocity. The energy increases however for $x > \mu$, which means that the term $(x-\mu)\dot{x}$ induces accelerated a movement. This interplay between energy dissipation and uptake is typical for adaptive systems.[5]

Fixpoints and Jacobian The Taken–Bogdanov system (2.33) has two fixpoints $(x^*, 0)$, with $x^* = 0, 1$. The eigenvalue of the Jacobian,

$$J = \begin{pmatrix} 0 & 1 \\ (1-2x^*) & (x^*-\mu) \end{pmatrix}, \qquad \begin{array}{l} \lambda_\pm(0,0) = \quad -\mu/2 \pm \sqrt{\mu^2/4 + 1} \\ \lambda_\pm(1,0) = (1-\mu)/2 \pm \sqrt{(1-\mu)^2/4 - 1} \end{array}$$

[5] Per definition, adaption implies that a system may both dissipate energy and increase its own reservoir, as discussed further in Sect. **??** of Chap. **??**, "**??**".

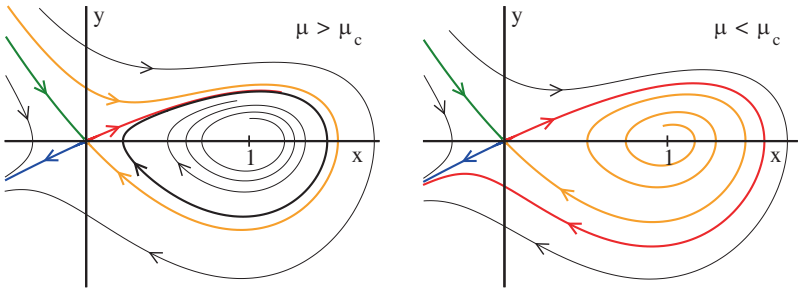

Fig. 2.12 The flow for the Taken–Bogdanov system (2.33). **Left:** The flow in the subcritical region, for $\mu = 0.9 > \mu_c \approx 0.8645$, together with the resulting limit cycle (thick black line). For $\mu \to \mu_c$ the unstable (red) and stable (orange) manifold join to form a homoclinic loop, which is identical to the locus of the limit cycle for $\mu \to \mu_c$. **Right:** The flow in the supercritical region, for $\mu = 0.8 < \mu_c$. The limit cycle did break after touching the saddle at $(0, 0)$.

show that $(0, 0)$ is always a saddle, a consequence of the quadratic maximum of mechanical potential $V(x)$ at $x = 0$.

The local minimum $(1, 0)$ of the potential is a stable/unstable focus for $\mu > 1$ and $\mu < 1$ respectively, with $\mu = 1$ being the locus of a supercritical Hopf bifurcation. We consider now $\mu \in [0, 1]$ and examine the further evolution of the resulting limit cycle.

Escaping the Potential Well We consider a particle starting with a vanishing velocity close to $x = 1$, the local minimum of the Potential well.

When the particle takes up enough energy from the environment, due to the velocity dependent force $(x - \mu)v$, it may be able to reach the local maximum at $x = 0$ and escape to $x \to -\infty$. This is the case when $\mu < \mu_c \approx 0.8645$. All orbits will escape when the region of energy uptake did expand to μ_c.

The particle remains trapped in the local potential well if dissipation dominates, which is the case for $\mu > \mu_c$. The particle is both trapped in the local well and repelled, at the same time, from the unstable minimum at $x = 1$, when $\mu_c < \mu < 1$. The orbit is forced in this case to perform an oscillatory motion around $x = 1$, which is equivalent to a stable limit cycle. This limit cycle increases in size for decreasing μ, exactly touching $(0, 0)$ for $\mu = \mu_c$, breaking apart byond, when $\mu < \mu_c$.

The bifurcation occurring at $\mu = \mu_c$ depends non-locally on the overall energy balance, as illustrated in Fig. 2.12. The "homoclinic transition" taking place in the Taken–Bogdanov system is therefore an example of a global bifurcation.

Homoclinic Bifurcation With a "homocline" one denotes a loop formed by joining a stable and an unstable manifold of the same fixpoint. Homoclines may generically only occur if either forced by symmetries or for special

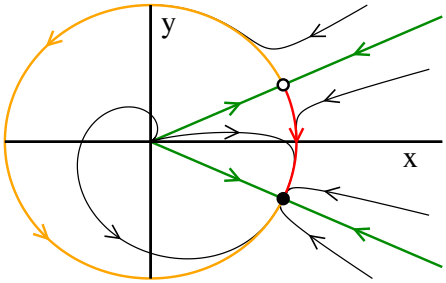

Fig. 2.13 The flow for a system showing an infinite period bifurcation, as defined by (2.35) and (2.36). Here $K = 1.1$. The stable fixpoint (filled circle) merges with the saddle (open cicle) in the limit $K \to 1$, which leads to a saddle-node bifurcation on an invariant cycle.

values of bifurcation parameters, with the later being the case for the Taken–Bogdanov system, which undergoes a homoclinic bifurcation.

An unstable and a stable manifold cross at $\mu = \mu_c$, compare Figs. 2.11 and 2.12, forming a homocline. The homocline is also the endpoint of the limit cycle present for $\mu > \mu_c$, which disappears for $\mu < \mu_c$. The limit cycle is hence destroyed at the point of its maximal size for a homoclinic bifurcation, and not when vanishing, as for a supercritical Hopf bifurcation.

2.3.1 Infinite Period Bifucation

For a further example of how a limit cycle may disappear discontinuously we consider two coupled oscillators characterized by their individual phases, respectively θ_1 and θ_2.[6]. A typical evolution equation for the phase difference $\varphi = \theta_1 - \theta_2$ is

$$\dot{\varphi} = 1 - K\cos(\varphi)\,. \tag{2.35}$$

We can interpret (2.35) via

$$\dot{r} = \left(1 - r^2\right) r, \qquad x = r\cos(\varphi), \qquad y = r\sin(\varphi) \tag{2.36}$$

within the context of a two dimensional limit cycle, compare (2.2).

The phase difference φ continuously increases for $|K| < 1$, with the system settling into a limit cycle. For $|K| > 1$ two fixpoints for $\dot{\varphi} = 0$ appear, a saddle and a stable node, as illustrated in Fig. 2.13. At this point, which correspond to a saddle-node bifurcation on an invariant cycle, the limit cycle breaks up.

Infinite Period Bifurcation The limit cycle for $|K| < 1$ has a revolution period T of

$$T = \int_0^T dt = \int_0^{2\pi} \frac{dt}{d\varphi} d\varphi = \int_0^{2\pi} \frac{d\varphi}{\dot{\varphi}} = \int_0^{2\pi} \frac{d\varphi}{1 - K\cos(\varphi)} = \frac{2\pi}{\sqrt{1 - K^2}}\,,$$

[6] This formulation parallels the Kuramoto model, which is treated detail in Sect. ?? of Chap. ??, "??".

which diverges in the limit $|K| \to 1$. The transition occurring at $|K| = 1$ is hence a "infinite period bifurcation", being characterized by a diverging time scale.

2.3.2 Catastrophe Theory

A catchy terminology for potentially discontinuous bifurcations in dynamical systems is "catastrophe theory", especially when placing emphasis on a geometric interpretation. Catastrophe theory is interested in bifurcations with "codimension" two or higher.

CODIMENSION The degrees of freedom characterizing a bifurcation diagram.

The codimension corresponds, colloquially speaking, to the number of parameters one may vary such that something interesting happens. The bifurcation normal forms discussed in Sect. 2.2.2 have a codimension of one.

Symmetry Broken Pitchfork Bifurcation We consider the one-dimensional system

$$\dot{x} = h + ax - x^3 \,. \tag{2.37}$$

For $h = 0$ the system reduces to the pitchfork normal form of (2.24), becoming invariant under the parity transformation $x \leftrightarrow -x$.

Parity is broken whenever $h \neq 0$. Eq. (2.37) can hence be used to study the influence of symmetry breaking onto a bifurcation diagram. There are two free parameters, h and a, the codimension is two.

Thermodynamic Phases The generalized pitchfork system (2.37) has a close relation to the theory of thermodynamic phase transitions, when assuming that

$$a = a(T) = a_0(T_c - T), \qquad a_0 > 0 \,,$$

where T is the temperature. In the absence of an external field h, only the trivial fixpoint $x^* = 0$ exists for $T > T_c$, viz for temperatures above the critical temperature T_c. In the ordered state, for $T < T_c$, there are two possible phases, characterized by the positive and negative stable fixpoints x^*.

Hysteresis and Memory The behavior of the phase transition changes when an external field h is present. Switching the sign of the field is accompanied, in the ordered state for $T < T_c$, by a "hysteresis-loop"

$$(1) \to (2) \to (3) \to (4) \to \ldots \,,$$

as illustrated in Fig. 2.14.

– The field h changes from negative to positive values along (1) → (2), with the fixpoint x^* remaining negative.

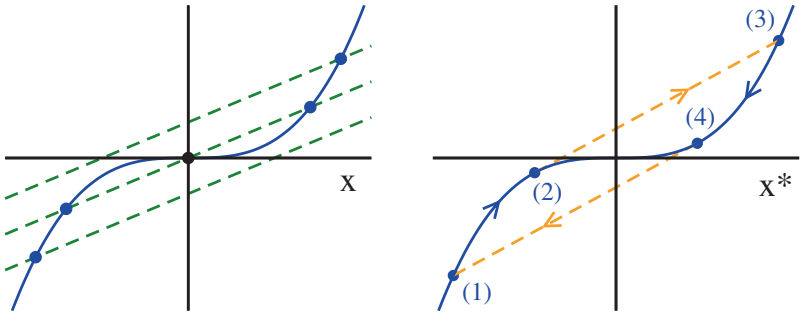

Fig. 2.14 Left: The self-consistency condition $x^3 = h + ax$ for the fixpoints x^* of the symmetry broken pitchfork system (2.37), for various fields h and a positive $a > 0$. The unstable fixpoint at $x = 0$ would becomes stable for $a < 0$, compare Fig. 2.9. **Right:** The hysteresis loop (1) → (2) → (3) → (4) → (1) occurring for $a > 0$ as function of the field h.

– At (2) the negative stable fixpoint disappears and the system makes a rapid transition to (3), the catastrophe.
– Lowering eventually again the field h, the system moves to (4), jumping in the end back to (1).

The system retains its state, x^* being positive or negative, to a certain extend and one speaks of a memory in the context of catastrophe theory.

Center Manifold A d-dimensional dynamical system with a fixpoint $\mathbf{x}^*$ and a Jacobian J,

$$\dot{\mathbf{x}} = \mathbf{f}(\mathbf{x}), \qquad J_{ij} = \frac{\partial f_i}{\partial x_j}\Big|_{\mathbf{x}=\mathbf{x}^*}, \qquad J\mathbf{e}_n = \lambda_n \mathbf{e}_n\,,$$

may have a number of neutral Lyapunov exponents with vanishing eigenvalues $\lambda_i = 0$ of the Jacobian.

CENTER MANIFOLD The space spanned by the neutral eigenvectors $\mathbf{e_i}$ is the center manifold.

Catastrophe theory deals with fixpoints having a non-vanishing center manifold.

Center Manifold of the Pitchfork System The Lyapunov exponent

$$\lambda = a - 3\,(x^*)^2$$

of the pitchfork system (2.37) vanishes at the jump-points (2) and (4) at which the catastrophe occurs, compare Fig. 2.14. At the jump-points $h + ax$ is per definition tangent to x^3, having identical slopes,

$$\frac{d}{dx}x^3 = \frac{d}{dx}\big(h + ax\big), \qquad 3x^2 = a\,. \tag{2.38}$$

At these transition points the autonomous flow becomes hence infinitesimally slow, since $\lambda \to 0$, a phenomenon called "critical slowing down" in the context of the theory of thermodynamic phase transitions.

Center Manifold Normal Forms The program of the catastrophe theory consists of finding and classifying the normal forms for the center manifolds of stationary points $\mathbf{x}^*$, by expanding to the next, non-vanishing order in $\delta\mathbf{x} = \mathbf{x} - \mathbf{x}^*$. The aim is hence to classify the types of dynamical behavior potentially leading to discontinuous transitions.

Catastrophic Fixpoints A generic fixpoint $\mathbf{x}^* = \mathbf{x}^*(\mathbf{c})$ may depend on control parameters $\mathbf{c} = (c_i, .., c_S)$ of the equations of motion, with S being the codimension. The flow is however smooth around a generic fixpoint and a finite center manifold arises only for certain sets $\{c_i^c\}$ of control parameters.

The controlling parameters of the pitchfork system (2.37) are h and a, in our example system, and a center manifold exists only when (2.38) is fulfilled, viz when

$$3\left[x^*(h^c, a^c)\right]^2 = a^c, \qquad x^*(h^c, a^c) = x_c^*$$

holds, which determines the set of "catastrophic fixpoints" x_c^*.

Changing the Controlling Parameters How does the location $\mathbf{x}^*$ of a fixpoint change upon variations $\delta\mathbf{c}$ around the set of parameters $\mathbf{c}^c$ determining the catastrophic fixpoint $\mathbf{x}_c^*$? With

$$\mathbf{x}_c^* = \mathbf{x}^*(\mathbf{c}^c), \qquad \mathbf{x}^* = \mathbf{x}^*(\mathbf{c}), \qquad \delta\mathbf{c} = \mathbf{c} - \mathbf{c}^c$$

we expand the fixpoint condition $\mathbf{f}(\mathbf{x}, \mathbf{c}) = 0$ and obtain

$$J\delta\mathbf{x}^* + P\delta\mathbf{c} = 0, \qquad J_{ij} = \frac{\partial f_i}{\partial x_j}, \qquad P_{ij} = \frac{\partial f_i}{\partial c_j}, \tag{2.39}$$

which we can invert if the Jacobian J is non-singular,

$$\delta\mathbf{x}^* = -J^{-1}P\delta\mathbf{c}, \qquad \text{if} \qquad |J| \neq 0\,. \tag{2.40}$$

The fixpoint may change however in a discontinuous fashion whenever the determinant $|J|$ of the Jacobian vanishes, viz in the presence of a center manifold. This is precisely what happens at a catastrophic fixpoint $\mathbf{x}_c^*(\mathbf{c}^c)$.

Catastrophic Manifold The set $\mathbf{x}_c^* = \mathbf{x}_c^*(\mathbf{c}^c)$ of catastrophic fixpoints is determined by two conditions, by the fixpoint condition $\mathbf{f} = 0$ and by $|J| = 0$. For the pitchfork system (2.37) we find,

$$a_c = 3\,(x_c^*)^2\,, \qquad h_c = (x_c^*)^3 - a_c x_c^* = -2\,(x_c^*)^3\,,$$

when using (2.38). Solving for $x_c^* = \sqrt{a_c/3}$ we can eliminate x_c^* and obtain

$$h_c = -2\,(a_c/3)^{3/2}\,, \qquad (h_c/2)^2 = (a_c/3)^3\,, \tag{2.41}$$

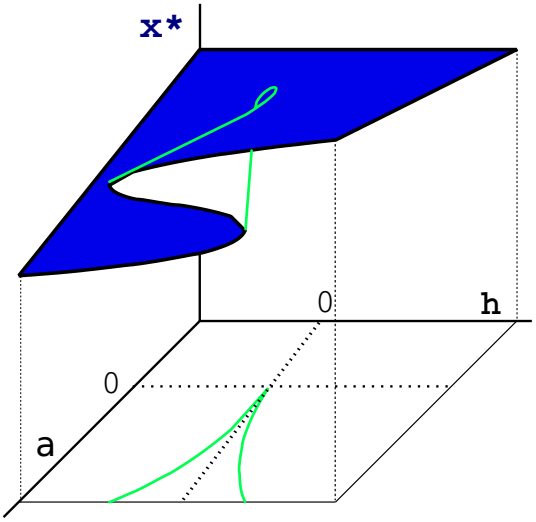

Fig. 2.15 The fixpoints x^* (upper folded plane) of the symmetry broken pitchfork system (2.37), as a function of the control parameters a and h. The catastrophic manifold (a_c, h_c), compare (2.41), has a cusp-like form (green lines).

which determines the "catastrophic manifold" (a_c, h_c) for the pitchfork transition, as illustrated in Fig. 2.15.

Classification of Perturbations The control parameters (a_c, h_c) of the pitchfork transition may be changed in two qualitatively distinct ways, namely along the catastrophic manifold (2.41), or perpendicular to it.

It would hence be useful to dispose of a list of canonical perturbations characterizing all possible distinct routes to change catastrophic fixpoints $x_c^* = x^*(\mathbf{c}^c)$ qualitatively, upon small changes $\delta\mathbf{c} = \mathbf{c} - \mathbf{c}^c$ of the control parameters $\mathbf{c}$. It is the aim of catastrophe theory to develop such a canonical classification scheme for the perturbations of center manifolds.

Gradient Dynamical Systems At times the flow $\mathbf{f}(\mathbf{x})$ of a dynamical system may be represented as a gradient of a bifurcation potential $U(\mathbf{x})$,

$$\dot{\mathbf{x}} = \mathbf{f}(\mathbf{x}) = -\nabla U(\mathbf{x})\,. \tag{2.42}$$

This is generically the case for one-dimensional systems, as discussed in Sect. 2.2.2, but otherwise not. For the gradient representation

$$\begin{aligned} \dot{x} &= g(x,y) \qquad & g &= -U_x(x,y) \\ \dot{y} &= h(x,y) \qquad & h &= -U_y(x,y) \end{aligned}$$

of a two-dimensional system to be valid, to give an example, the cross-derivatives $g_y = -U_{xy} = -U_{yx} = h_x$ would need to coincide. This is however normally not the case.

For gradient dynamical systems one needs to discuss only the properties of the bifurcation potential $U(\mathbf{x})$, as scalar quantity, and they are hence

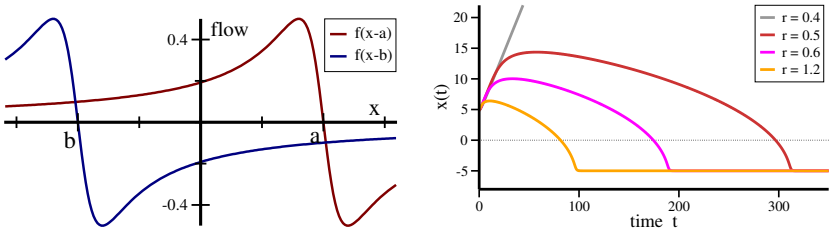

Fig. 2.16 Rate-induced tipping. **Left:** The fixpoints $x^* = a/b$ are stable for the individual flows (2.43), here for $a = 5$ and $b = -5$. The stationary points shift to $\pm\sqrt{5^2 - 1} \approx \pm 4.9$ when the two flows are superimposed, as given by (2.45). **Right:** The orbits $x(t)$ under the influence of a forcing $\dot{a} = r$. For small rates the system manages to adapt, as for $r = 0.4$, for larger rates not. For $r = 0.5/0.6/1.2$ the system tips towards the alternative steady state.

somewhat easier to investigate than a generic dynamical system of the form $\dot{\mathbf{x}} = \mathbf{f}(\mathbf{x})$. Catastrophe theory is mostly limited to gradient systems.

2.3.3 Rate Induced Tipping

For the bifurcation scenarios studied hitherto, we took as a precondition that controlling parameters changed slowly, on time scales substantially exceeding that of the primary dynamics. This is the "adiabatic limit".

Bifurcation vs. Tipping A rapid transfer between distinct stable manifolds may occur when systems reach a bifurcation point upon adiabatic parameter changes, as illustrated in Fig. 2.14. Systems undergoing self-accelerating instabilities are said "to tip", which is a somewhat broader terminology. Instead of a description in terms of an abstract bifurcation, 'tipping' emphasizes the role of positive feedback effects. This view is particulary important in climatology and ecology.

Rate Induced Tipping Individual components of a dynamical system may evolve on vastly different time scales. In climatology, a widely discussed slow component is the Greenland iceshield, which takes millenia to grow or melt. In ecology, adaption to changing enviromental condition via Darwinian evolution is likewise a slow process, extending over geological periods.[7] Systems with slow components may show a reduced resilence against shocks in terms of rapid parameter changes, as typical for climatic and ecological systems facing anthropogenic forcing. When the rate matters, at which control parameters change, "rated induced tipping" may occur.

[7] See Chap. **??**, "**??**".

Competing Fixpoints Close to an attracting state the flow is linear. At larger distances z, the numerical size of the flow $f = f(z)$ may however fade away, f.i. as described by

$$\dot{x} = f(x-a), \qquad f(z) = \frac{-z}{1+z^2}\,. \tag{2.43}$$

In this example the flow decays inversely with the distance to the fixpoint $x^* = a$, as illustrated in Fig. 2.16, after being maximal in magnitude at $x = a \pm 1$. For two attracting states the dynamics takes the form

$$\dot{x} = f(x-a) + f(x-b)\,, \tag{2.44}$$

which makes the system bistable. The two flows compete with each other, which shifts the two stable fixpoints,

$$(x-a)\big[1+(x-b)^2\big] = -(x-b)\big[1+(x-a)^2\big]\,,$$

as determined by $\dot{x} = 0$, or

$$(x-a)(x-b) = -1, \qquad x = \pm\sqrt{a^2-1}\,, \tag{2.45}$$

where we specialized in the last step to $b = -a$. The two stable fixpoints are sperated by an unstable fixpoint at $x = 0$. Eq. (2.44) describes a situation in which the influence of attracting states decays in phase space, which is typical for dynamical systems composed of interacting real-world identities. An example would be physical objects, whose sphere of influence is often limited to the immediate surrounding.

Adaption Catastrophy In (2.44) the dynamical variable $x = x(t)$ reflects the state of the system. In the following we take $x \approx a$ to correspond to a healthy system, say a pristine ecosystem, and states $x \approx b$ to a disrupted system. External impacts may change the control parameter $a = a(t)$, e.g. with a constant rate r,

$$\dot{a} = r\,.$$

The orbit cannot follow when a moves to the right too fast, which happens when $\dot{x} < \dot{a} = r$. Given that $f(x-a)$ is bounded, this necessarily happens with increasing r. At this point the system fails to adapt to the changing environment, with the orbit reverting to the disrupted state close to b. Rate induced tipping occurs in the form of an adaption catastrophy. Extended transients are observed close to the critical rate r, as shown in Fig. 2.16.

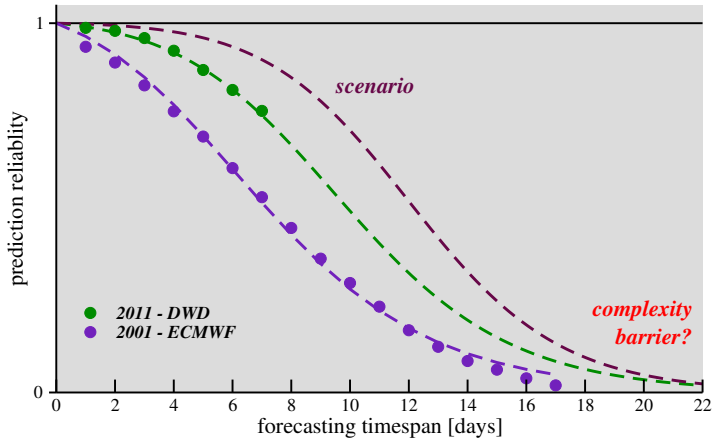

Fig. 2.17 The average accuracy of weather forecasting, normalized to $[0, 1]$, decreases rapidly with increasing prediction timespan, due to the chaotic nature of weather dynamics. Increasing the resources devoted for improving the prediction accuracy results in decreasing returns close to the resulting complexity barrier. Reprinted from **?** under CC-BY-4.0 license, © 2012 Complex Systems Publications, Inc.

2.4 Logistic Map and Deterministic Chaos

The notion of "chaos" plays an important role in dynamical systems theory. A chaotic system is defined as a system that cannot be predicted within a given numerical accuracy. At first sight this seems to be a surprising concept, since differential equations of the type of (2.15), which do not contain any noise or randomness, are perfectly deterministic. Once the starting point is known, the resulting trajectory can be calculated for all times. Chaotic behavior can arise nevertheless, due to an exponential sensitivity to initial conditions.

Deterministic Chaos A deterministic dynamical system is chaotic when it shows exponential sensibility with respect to initial conditions.

This means that a very small change in the initial setting can blow up even after a short time. When considering real-world applications, when models need to be determined from measurements containing inherent errors and limited accuracies, an exponential sensitivity can result in unpredictability. A well known example is the problem of long-term weather prediction, as shown in Fig. 2.17.

Logistic Map One of the most cherished models in the field of deterministic chaos is the logistic map of the interval $[0, 1]$ onto itself,

$$x_{n+1} = g(x_n) \equiv r\, x_n\, (1 - x_n), \qquad x_n \in [0, 1], \qquad r \in [0, 4]\,, \tag{2.46}$$

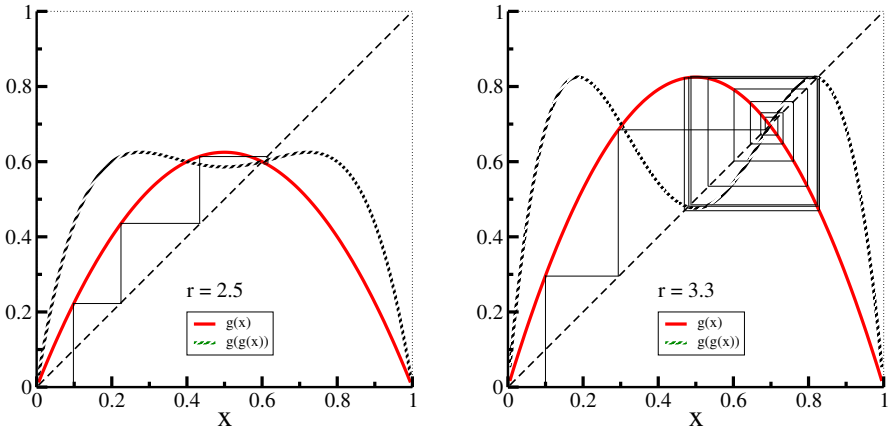

Fig. 2.18 The logistic map $g(x) = rx(1-x)$ (red), and the iterated logistic map $g(g(x))$ (green); for $r=2.5$ (left) and $r=3.3$ (right). Also shown are iterations of $g(x)$, starting from $x=0.1$ (thin solid line). Note, that the fixpoint $g(x) = x$ is stable/unstable for $r=2.5$ and $r=3.3$, respectively. The orbit is attracted to a fixpoint of $g(g(x))$ for $r=3.3$, corresponding to a cycle of period two for $g(x)$.

where we made use of the notation $x_n = x(n)$, for discrete times $n = 0, 1, \ldots$. The functional dependence is illustrated in Fig. 2.18. Despite its apparent simplicity, the logistic map shows an infinite series of bifurcations that culminate in a transition to chaos.

Biological Interpretation We may consider $x_n \in [0,1]$ as standing for the population density of a reproducing species in the year n. In this case the factor $r(1-x_n) \in [0,4]$ corresponds to the number of offspring per year and animal, which is limited for high population densities $x \to 1$, viz when resources become scarce. The classical example is that of a herd of reindeer on an island.

Knowing the population density x_n in a given year n we may predict via (2.46) the population density for all subsequent years exactly; the system is deterministic. Nevertheless the population shows irregular behavior for certain values of r, which is hence chaotic.

Fixpoints of the Logistic Map We start with the fixpoints of $g(x)$,

$$x = rx(1-x) \qquad \Longleftrightarrow \qquad x = 0 \quad \text{or} \quad 1 = r(1-x)\,.$$

The non-trivial fixpoint is

$$1/r = 1 - x, \qquad x^{(1)} = 1 - 1/r, \qquad r_1 < r, \qquad r_1 = 1\,. \tag{2.47}$$

It is present for $r_1 < r$, with $r_1 = 1$, due to the restriction $x^{(1)} \in [0,1]$.

Stability Analysis For maps, fixpoints are stable when the derivative g' of the flow is smaller than one in magnitude, see (2.14). For $x^{(1)} = 1 - 1/r$ this translates to

$$g'(x) = r(1-2x), \qquad g'\big(x^{(1)}\big) = 2 - r\,. \tag{2.48}$$

Noting that $r \in [1,4]$, we obtain

$$|2-r| < 1 \quad \Longleftrightarrow \quad r_1 < r < r_2 \qquad \text{with} \quad \begin{cases} r_1 = 1 \\ r_2 = 3 \end{cases} \tag{2.49}$$

for the region of stability of $x^{(1)}$.

Fixpoints of Period Two For $r > 3$ a fixpoint of period two appears. This fixpoint is is a fixpoint of the iterated function

$$g(g(x)) = rg(x)(1-g(x)) = r^2 x(1-x)(1-rx(1-x))\,.$$

The fixpoint equation $x = g(g(x))$ leads to the cubic equation

$$\begin{aligned} 1 &= r^2(1 - rx + rx^2) - r^2 x(1 - rx + rx^2), \\ 0 &= r^3x^3 - 2r^3x^2 + (r^3 + r^2)x + 1 - r^2\,. \end{aligned} \tag{2.50}$$

In order to find the roots of (2.50) we use the fact that $x = x^{(1)} = 1 - 1/r$ is a stationary point of both $g(x)$ and $g(g(x))$, see Fig. 2.18. Dividing (2.50) by the root $(x - x^{(1)}) = (x - 1 + 1/r)$ one obtains

$$\begin{gathered} (r^3x^3 - 2r^3x^2 + (r^3 + r^2)x + 1 - r^2) : (x - 1 + 1/r) \;= \\ r^3x^2 - (r^3 + r^2)x + (r^2 + r)\,. \end{gathered}$$

The two fixpoints of $g(g(x))$ are therefore the roots of

$$x^2 - \left(1 + \frac{1}{r}\right) x + \left(\frac{1}{r} + \frac{1}{r^2}\right) = 0\,,$$

which leads to

$$x_{\pm}^{(2)} = \frac{1}{2}\left(1 + \frac{1}{r}\right) \pm \sqrt{\frac{1}{4}\left(1 + \frac{1}{r}\right)^2 - \left(\frac{1}{r} + \frac{1}{r^2}\right)}\,. \tag{2.51}$$

Period Doubling Bifurcation We have three fixpoints of period two for $r > 3$ (two stable ones and one unstable), and only a single fixpoint for $r < 3$. What happens at $r = 3$?

$$\begin{aligned} x_{\pm}^{(2)}(r=3) &= \frac{1}{2}\frac{3+1}{3} \pm \sqrt{\frac{1}{4}\left(\frac{3+1}{3}\right)^2 - \left(\frac{3+1}{9}\right)} \\ &= \frac{2}{3} = 1 - \frac{1}{3} = x^{(1)}(r=3)\,. \end{aligned}$$

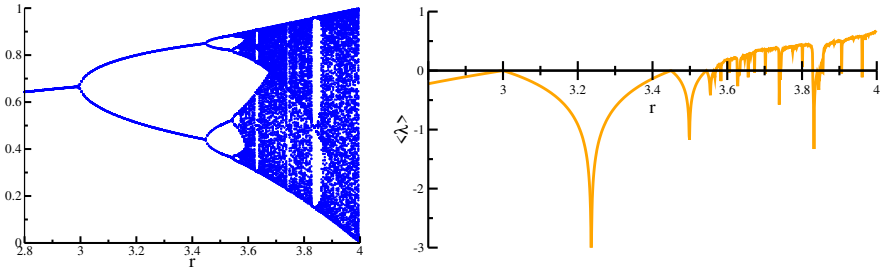

Fig. 2.19 Left: The values x_n for the iterated logistic map (2.46). For $r < r_\infty \approx 3.57$ the x_n go through cycles with finite but progressively longer periods. For $r > r_\infty$ the plot would be fully covered in most regions if all x_n would be shown. **Right:** The corresponding maximal Lyapunov exponents, as defined by (2.55). Positive Lyapunov exponents λ indicate chaotic behavior.

At $r = 3$ the fixpoint splits into two stable and one unstable branch, see Fig. 2.19, akin to the pitchfork bifurcations discussed in Sect. 2.2. Given that a period doubling occurs at $r = 3$, the transition can be seen alternatively as the discrete analog of a supercritical Hopf bifurcation.

Bifurcation Cascade One may carry out a stability analysis for $x_\pm^{(2)}$, just as for $x^{(1)}$. One finds a critical value $r_3 > r_2$ such that

$$x_\pm^{(2)}(r) \;\text{ stable} \qquad \Longleftrightarrow \qquad r_2 < r < r_3\,. \tag{2.52}$$

Going further on one finds an r_4 such that there are four fixpoints of period four, that is of $g(g(g(g(x))))$, for $r_3 < r < r_4$. In general there are critical values r_n and r_{n+1} such that there are

$$2^{n-1} \;\text{ fixpoints } x^{(n)} \text{ of period } 2^{n-1} \qquad \Longleftrightarrow \qquad r_n < r < r_{n+1}\,.$$

The logistic map therefore shows iterated bifurcations. This, however, is not yet chaotic behavior.

Chaos in the Logistic Map There exists a critical r_∞ at which the period-doubling series converges,

$$\lim_{n\to\infty} r_n \;\to\; r_\infty, \qquad r_\infty = 3.5699456\ldots$$

No stable fixpoint of even period exists in the region

$$r_\infty \;<\; r \;<\; 4\,.$$

In order to characterize the sensitivity of (2.46) with respect to the initial condition, we consider two slightly different starting points x_1 and x_1':

$$x_1 - \;x_1' = y_1, \qquad |y_1| \;\ll\; 1\,.$$

The key question is then whether the difference

$$y_m = x_m - \ x'_m, \qquad y_{m+1} \approx \frac{dg(x)}{dx}\Big|_{x=x_m} y_m \tag{2.53}$$

between the two respective orbits is still small after m iterations. For (2.53) we used $x'_m = x_m - y_m$, neglecting terms $\sim y_m^2$. We hence obtain

$$y_{m+1} = r(1-2x_m)\, y_m \equiv \epsilon\, y_m \,.$$

For $|\epsilon| < 1$ the map is stable, as two initially different populations close in with time passing. For $|\epsilon| > 1$ they diverge; the map is chaotic.

Lyapunov Exponents We remind ourselves of the definition

$$|\epsilon| = \mathrm{e}^{\lambda}, \qquad \lambda = \log \left| \frac{dg(x)}{dx} \right| \tag{2.54}$$

the Lyapunov exponent $\lambda = \lambda(r)$ of a map, as introduced in Sect. 2.2. For positive Lyapunov exponents the time development is exponentially sensitive to the initial conditions and shows chaotic features,

$$\lambda < 0 \ \Leftrightarrow \ \text{stability}, \qquad \lambda > 0 \ \Leftrightarrow \ \text{instability}\,.$$

This is indeed observed in nature, e.g. for populations of reindeer on isolated islands, as well as for the logistic map for $r_\infty < r < 4$, compare Fig. 2.19.

Maximal Lyapunov Exponent The Lyapunov exponent, as defined by (2.54), provides a description of the short time behavior. For a corresponding characterization of the long time dynamics one defines the "maximal Lyapunov exponent"

$$\lambda^{(\max)} = \lim_{n \gg 1} \frac{1}{n} \log \left| \frac{dg^{(n)}(x)}{dx} \right|, \qquad g^{(n)}(x) = g(g^{(n-1)}(x))\,. \tag{2.55}$$

Using (2.54) for the short time evolution we can decompose $\lambda^{(\max)}$ into an averaged sum of short time Lyapunov exponents. $\lambda^{(\max)}$ is the "global Lyapunov exponent".

One needs to select advisedly the number of iterations n in (2.55). On one side n should be large enough such that short-term fluctuations of the Lyapunov exponent are averaged out. The available phase space is however generically finite, for the logistic map we have $y \in [0,1]$. Therefore, two initially close orbits cannot diverge ad infinitum. One needs hence to avoid phase-space restrictions, evaluating $\lambda^{(\max)}$ for large but finite numbers of iterations n.

Routes to Chaos The chaotic regime $r_\infty < r < 4$ of the logistic map connects to the regular regime $0 < r < r_\infty$ with increasing period doubling.

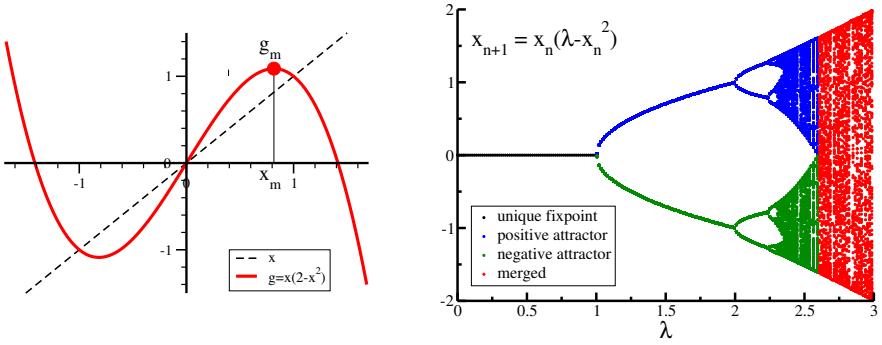

Fig. 2.20 **Left:** For $\lambda = 2$, the odd logistic map (2.56). The local maximum g_m is reached for $x_m = \sqrt{\lambda/3} \approx 0.82$. **Right:** The bifurcation diagram of the odd logistic map as a function of λ. One has a unique fixpoint $x_n = 0$ (black) for $\lambda < 1$ and two equivalent attractors (blue/green) for $1 < \lambda < \lambda_s$, which merge at $\lambda_s = \sqrt{27}/2 \approx 2.6$. Inversion symmetry is restored at λ_s (red). A period-doubling transition to chaos is observable in the symmetry broken phase.

One speaks of a "route to chaos via period-doubling". The study of chaotic systems is a wide field of research and a series of routes leading from regular to chaotic behavior have been found. Two important alternative routes to chaos are:

- Intermittency route to chaos
  The trajectories are almost periodic and interdispersed with regimes of irregular behaviour. The occurrence of these irregular bursts increases until the system becomes irregular.
- Ruelle–Takens–Newhouse route to chaos
  A strange attractor appears in a dissipative system after two (Hopf) bifurcations. As a function of an external parameter a fixpoint evolves into a limit cycle (Hopf bifurcation), which then turns into a limiting torus, which subsequently turns into a strange attractor.

2.4.1 Colliding attractors

Bifurcations are generically the result of colliding invariant manifolds, viz of stable and unstable fixpoints, limit cycles and chaotic sets. Examples are the saddle-node bifurcation (2.19), at which a stable and an unstable fixpoint merge, and the collision between a limit cycle and a saddle within the Taken–Bogdanov system (2.33).

Odd Logistic Map The collision between two chaotic attractors can be studied within the odd logistic map

$$x_{n+1} = g(x_n) = x_n\big(\lambda - x_n^2\big), \qquad \lambda > 0\,, \tag{2.56}$$

which is invariant under inversion $x \leftrightarrow (-x)$. The local maximum $g_m = g(x_m)$ is given by

$$g' = 0, \qquad x_m = \sqrt{\frac{\lambda}{3}}, \qquad g_m = 2\sqrt{\frac{\lambda^3}{3^3}}\,, \tag{2.57}$$

as illustrated in Fig. 2.20.

Merging Chaotic Attranctors For $\lambda < 1$ only the trivial fixpoint exists. Afterwards, for $1 < \lambda < \lambda_s$, there are two attracting states that are related via inversion symmetry, as shown in Fig. 2.20. Both branches undergo a period-double transition to chaos, in equivalence to the one observed for the standard logistic map, compare Fig. 2.19. At λ_s, determined by

$$g(g_m) = 0, \qquad \lambda_s = 4\,\frac{\lambda_s^3}{3^3}, \qquad \lambda_s = \frac{\sqrt{27}}{2}\,, \tag{2.58}$$

the two attractors merge. Only a single chaotic attractor remains for $\lambda > \lambda_s$.

Chaotic Attractors in Crisis In general, different types of attractors may collide. A Hopf bifurcation, f.i., occurs when limit cycles contract to a point, which is equivalent to the merger of limit cycles with fixpoints. One speaks of a "crisis" when chaotic attractors collide with unstable fixpoints or limit cycles. For the logistic map (2.46), a crisis occurs at $r = 4$, namely when the chaotic attractor hits the unstable fixpoint $x = 0$. Orbits diverge for $r > 4$.

2.5 Dynamical Systems with Time Delays

The dynamical systems we considered so far all had instantaneous dynamics, being of the type

$$\begin{aligned} \frac{d}{dt}y(t) &= f(y(t)), \qquad t > 0 \\ y(t=0) &= y_0\,, \end{aligned} \tag{2.59}$$

when denoting with y_0 the initial condition. This is the simplest case: one dimensional (a single dynamical variable only), autonomous ($f(y)$ is not an explicit function of time) and deterministic (no noise).

Time Delays In many real-world applications the couplings between different subsystems and dynamical variables is not instantaneous. Signals and physical interactions need a certain time to travel from one subsystem to the next. Time delays are therefore encountered commonly and become important when the delay time T is comparable to the intrinsic time scales of the dynamical system. We consider here the simplest case, a noise-free one-

dimensional dynamical system with a single delay time,

$$\frac{d}{dt}y(t) = f(y(t), y(t-T)), \qquad t > 0 \tag{2.60}$$
$$y(t) = \phi(t), \qquad t \in [-T, 0]\,.$$

Due to the delayed coupling we need now to specify an entire initial function $\phi(t)$. Differential equations containing one or more time delays need to be considered carefully, with the time delay introducing additional dimensions to the problem. We discuss a several basic examples.

Linear Couplings We start with the linear delay equation

$$\frac{d}{dt}y(t) = -ay(t) - by(t-T), \qquad a, b > 0\,. \tag{2.61}$$

The only constant solution for $a + b \neq 0$ is the trivial state $y(t) \equiv 0$. The trivial solution is stable in the absence of time delays, $T = 0$, whenever $a + b > 0$. The question is, whether a finite T may change this.

We may expect the existence of a certain critical T_c, such that $y(t) \equiv 0$ remains stable for small time delays $0 \leq T < T_c$. In this case the initial function $\phi(t)$ will affect the orbit only transiently, in the long run the motion would be damped out, approaching the trivial state asymptotically for $t \to \infty$.

Delay Induced Hopf Bifurcation Trying our luck with the usual exponential ansatz, we find

$$\lambda = -a - b\mathrm{e}^{-\lambda T}, \qquad y(t) = y_0\mathrm{e}^{\lambda t}, \qquad \lambda = p + iq\,. \tag{2.62}$$

Separating into a real and an imaginary part we obtain

$$\begin{aligned} p + a &= -b\mathrm{e}^{-pT}\cos(qT), \\ q &= b\mathrm{e}^{-pT}\sin(qT)\,. \end{aligned} \tag{2.63}$$

For $T = 0$ the solution is $p = -(a + b)$, $q = 0$, as expected, and the trivial solution $y(t) \equiv 0$ is stable. A numerical solution is shown in Fig. 2.21 for $a = 0.1$ and $b = 1$. The crossing point $p = 0$ is determined by

$$a = -b\cos(qT), \qquad q = b\sin(qT)\,. \tag{2.64}$$

The first condition in (2.64) can be satisfied only for $a < b$. Taking the squares in (2.64) and eliminating qT one has

$$q = \sqrt{b^2 - a^2}, \qquad T \equiv T_c = \arccos(-a/b)/q\,.$$

One therefore finds a Hopf bifurcation at $T = T_c$, which implies that the trivial solution becomes unstable for $T > T_c$. For $a = 0$ the transition point is defined by $q = b$, together with $T_c = \pi/(2b)$. Note, that there is a Hopf

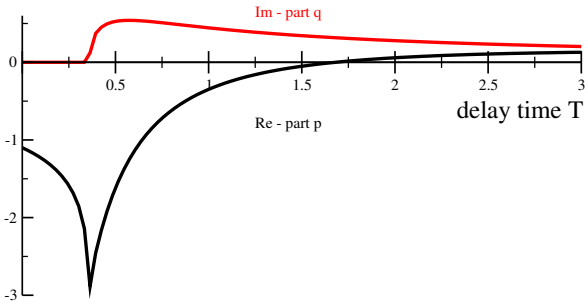

Fig. 2.21 For $a = 0.1$ and $b = 1$, the components p and q of the solution $\mathrm{e}^{(p+iq)t}$ of the delay system given by (2.61). The state $y(t) \equiv 0$ becomes unstable whenever the real part p turns positive. The imaginary part q is given in units of π.

bifurcation only for $a < b$, viz whenever the time delay dominates, and that q becomes non-zero well before the bifurcation point, compare Fig. 2.21. One has therefore a region of damped oscillatory behavior with $q \neq 0$ and $p < 0$.

Discontinuities For differential equations with time delays one may specify arbitrary initial functions $\phi(t)$, also initial functions with discontinuities, which will induce discontinuities in the derivatives of the respective trajectories. As an example we consider the case $a = 0$, $b = 1$ of (2.61), with a non-zero constant initial function,

$$\frac{d}{dt}y(t) = -y(t-T), \qquad \phi(t) \equiv 1\,. \tag{2.65}$$

The solution can be evaluated by stepwise integration,

$$y(t) - y(0) = \int_0^t dt' \dot{y}(t') = -\int_0^t dt' y(t'-T) = -\int_0^t dt' = -t,\ 0 < t < T\,.$$

The first derivative in consequently discontinuous at $t = 0$,

$$\lim_{t\to 0-} \frac{d}{dt}y(t) = 0, \qquad \lim_{t\to 0+} \frac{d}{dt}y(t) = -1\,.$$

In analogy one show that the second derivative has a discontinuity at $t = T$, the third derivative at $t = 2T$, and so on.

Injectivity Ordinary differential equations are injective in the sense that distinct initial conditions lead to distinct trajectories. This holds regardless of the presence of attracting manifolds, which determine solely the long-term behavior.

Delay systems are not necessarily injective with respect to the initial function. Consider logistic growth with a delayed growth rate,

$$\frac{d}{dt}y(t) = y(t-T)\big(y(t)-1\big), \qquad \phi(t=0) = 1\,. \tag{2.66}$$

For any $\phi(t)$ with $\phi(0) = 1$ the solution is $y(t) \equiv 1$ for all $t \in [0, \infty]$. Distinct initial functions lead to identical orbits.

Non-Constant Time Delays Things may become rather weird when the time delays are not constant, as for

$$\begin{aligned} \tfrac{d}{dt}y(t) &= y\big(t - T(y)\big) + \tfrac{1}{2}, \qquad T(y) = 1 + |y(t)|, \\ \phi(t) &= \begin{cases} 1 & t < -1 \\ 0 & t \in [-1, 0] \end{cases} . \end{aligned} \tag{2.67}$$

It is easy to see, that the two functions

$$y(t) = \frac{t}{2}, \qquad y(t) = \frac{3t}{2}, \qquad t \in [0, 2]\,,$$

are both solutions of (2.67), with appropriate continuations for $t > 2$. Two different solutions of the same differential equation and identical initial conditions, this cannot happen for ordinary differential equations. It is evident, that special care must be taken when examining dynamical systems with time delays numerically.

2.5.1 Distributed time delays

Basic delay differential systems contain a single time delay T, like (2.61), which corresponds to an instanteous memory process. In general, the memory $y_M(t)$ of past trajectories will be a convolution,

$$y_M(t) = \int_0^\infty K(\tau) y(t - \tau) d\tau, \qquad \int_0^\infty K(\tau) d\tau = 1\,, \tag{2.68}$$

where we defined with $K(\tau)$ the delay kernel. For a sharply peaked delay kernel, $K(\tau) = \delta(\tau - T)$, one recovers $y_M(t) = y(t - T)$.

Exponentially Distributed Delays Explicitly we consider with

$$K(\tau) = \frac{1}{T}\,\mathrm{e}^{-\tau/T} \tag{2.69}$$

exponentially distributed time delays. One has

$$\frac{d}{dt}y_M(t) = \int_0^\infty d\tau K(\tau)\frac{d}{dt}y(t - \tau) = -\int_0^\infty d\tau K(\tau)\frac{d}{d\tau}y(t - \tau), \tag{2.70}$$

which allows to integrate the last expression by parts when using (2.69). The resulting closed expression,

$$\dot{y}_M = \frac{-1}{T} \int_0^\infty d\tau \mathrm{e}^{-\tau/T} \frac{d}{d\tau} y(t-\tau) = \frac{y - y_M}{T} \,, \tag{2.71}$$

corresponds to a trailing average, with the memory variable y_M trying to approach y.

Kernel Series Framework Eq. (2.71) implies that a delay differential equation with exponentially distributed delays can be mapped exactly to a system of ordinary differential equations by adding an additional variable, namely $y_M(t)$. For generic kernels $K(\tau)$ in (2.68) one can generalize this concept by adding a diverging number of memory variables. With this approach, denoted "kernel series framework", one can map any time delay system to a N-dimensional system of ordinary differential equations. For the case of a single time delay one speaks of the "linear chain trick". In general one has $N \to \infty$, which reflects the notion that delay stystems are formaly infinite dimensional.